Osteoporosis International (2022) 33:1309–1321
https://doi.org/10.1007/s00198-021-06288-5

ORIGINAL ARTICLE

Age-related reference data of bone microarchitecture, volumetric bone density, and bone strength parameters in a population of healthy Brazilian men: an HR-pQCT study

J.C. Alvarenga[1] · V.F. Caparbo[1] · D.S. Domiciano[1] · R.M.R. Pereira[1]

Received: 9 August 2021 / Accepted: 21 December 2021 / Published online: 20 January 2022

Abstract

Summary In a cross-sectional cohort of 340 healthy Brazilian men aged 20 to 92 years, data on density, structure, and strength of the distal radius and tibia were obtained using high-resolution peripheral quantitative computed tomography (HR-pQCT) to develop age- and site-specific reference curves. Age-dependent changes differed between the sites and bone compartments (trabecular and cortical).

Introduction The aim of this study was to establish age-related reference curves for bone densities, microarchitectural properties, and estimated failure load measured by HR-pQCT (distal radius and tibia) in men. Also, to correlate bone stiffness with the other HR-pQCT parameters, areal bone mineral density (BMD) by DXA and trabecular bone score (TBS).

Methods Healthy Brazilian men ($n = 340$) between the ages of 20 and 92 years were recruited. Non-dominant radius and left tibia were scanned using HR-pQCT (Xtreme CT I). Standard and automated segmentation methods were performed, and bone strength estimated by FE analysis. Bone mineral density at lumbar spine, total hip, femoral neck, and TBS were measured using DXA (Hologic, QDR4500).

Results Age-related reference curves were constructed at the distal radius and tibia for volumetric bone density, morphometry, and estimated bone strength parameters. There was a linear relationship with age only for thickness measurements of distal radius (trabecular: R^2 0.108, $p<0.001$; cortical: R^2 0.062, $p=0.002$) and tibia (trabecular: R^2 0.109, $p<0.001$; cortical: R^2 0.063, $p=0.010$), and bone strength at distal radius (R^2 0.157, $p<0.001$). The significant correlations ($p<0.05$) found by Pearson's correlations (r) between bone stiffness and all other variables measured by HR-pQCT and DXA showed to be stronger at the tibia site than the distal radius.

Conclusion The current study expands the HR-pQCT worldwide database and presents an adequate methodology for the construction of reference data in other populations. Moreover, the correlation of bone strength estimated by FEA with other bone microstructural parameters provided by HR-pQCT helps to determine the contribution of each of these variables to fracture risk prediction in men.

Keywords Age-related bone loss · Bone strength · High-resolution peripheral computed tomography · Reference values

Introduction

Bone is a dynamic tissue, and the formation and resorption are continuous processes during life [1]. Osteoporosis and fractures are important complications of aging in men. According to the National Osteoporosis Foundation, up to 25% of men over the age of 50 years will experience a fracture due to osteoporosis [2]. In 2050, the incidence of hip fracture in men is expected to increase by 310% worldwide [3]. Moreover, men suffering from any major fracture have a higher mortality rate than women [4]. Indeed, the lifetime risk of experiencing an osteoporotic fracture in Caucasian men is 13% and is greater than the lifetime risk of developing another frequent cause of morbimortality in men: prostate cancer (11.3%) [5, 6].

Currently, measurement of the areal bone mineral density (aBMD) in the lumbar spine and femoral neck using

✉ R.M.R. Pereira
rosamariarp@yahoo.com

[1] Bone Metabolism Laboratory, Rheumatology Division, Hospital das Clinicas HCFMUSP, Faculdade de Medicina, Universidade de Sao Paulo, Av Dr Arnaldo, 455, 3° andar, sala 3193, Sao Paulo, SP 01246-903, Brazil

dual-energy X-ray absorptiometry (DXA) is most commonly used to diagnose osteoporosis and assess bone quantity and changes in bone mass across the life span [7]. DXA measurements are an indirect surrogate for bone strength and have some limitations on distinguishing patients at low and high fracture risk [7, 8]. For instance, it can neither discriminate between cortical and trabecular bones nor evaluate bone microarchitecture [9].

Trabecular bone score (TBS) is a measurement that can be applied to DXA images. It is a gray-level textural index of bone architecture derived from lumbar spine DXA images and is an independent indicator of fracture risk [10]. Additionally, TBS is an important determinant of bone strength [11]. The association of TBS with incident clinical fractures in men has been consistently estimated in two previous cohorts [11, 12].

High-resolution peripheral quantitative computed tomography (HR-pQCT) is a technology that provides three-dimensional images allowing assessment of volumetric bone density and bone microarchitecture components in the examined area [8, 13]. After the acquisition of standard and automated segmentation methods, dedicated finite element (FE) analysis provides a direct subject-specific estimation of bone strength [14–19].

Prior studies on HR-pQCT have not concomitantly evaluated bone features using different technologies, which is essential for determining the contribution of each one to fracture risk prediction in adult men [8, 16, 19–24]. Furthermore, no study has evaluated bone by HR-pQCT in men from Latin America. As the availability of HR-pQCT increases with a growing number of health professionals having access to the technology, there is an unmet need to establish reference data that can be used as a basis for assessing bone health in different populations.

The primary objective of the present cross-sectional study was to (a) establish age-related reference values for volumetric bone density and morphometry by HR-pQCT and FE parameters of distal radius and tibia, in a healthy male population, and (b) correlate bone stiffness of distal radius and tibia with other HR-pQCT parameters, areal BMD and TBS.

Methods

Participants

A total of 340 healthy men aged 20 to 92 years were enrolled in the study. This population included workers from the University of São Paulo School of Medicine, Hospital das Clinicas of the University of São Paulo, or family members of the employees. At least 40 subjects per decade of age were recruited. Exclusion criteria were bone-associated metabolic disease (rickets, primary hyperparathyroidism, osteomalacia, and Paget's disease), prior non-traumatic fracture, chronic disease (diabetes mellitus, renal or liver failure, hyperthyroidism, hypothyroidism, and malabsorption), use of any medication that interferes with bone metabolism (bisphosphonates, teriparatide, glucocorticoids, anticonvulsants, anticoagulants), current smoking (tobacco use), and alcohol intake $\geq$ 3 U/day.

This study was approved by the Local Ethics in Research Committee of the São Paulo University School of Medicine, and all participants gave written informed consent.

Data collection

Demographic and anthropometric characteristics, including race, age, height, weight, and body mass index (BMI) were recorded. Race was defined based on self-reporting of the second generation of ancestors, an approach previously used for the Brazilian population [25, 26]. Individuals who reported having four White grandparents were classified as White. Individuals with black African and White ancestry (mixed race) were classified as non-White. When racial information on an individual's grandparents was not available, the race of an individual was determined by the race of his parents. The descendants of other races were not included. All the participants underwent a standardized interviewer-administered questionnaire that ascertained clinical characteristics, including smoking (tobacco use) status, alcohol consumption, physical activity (including work activities), previous non-vertebral fracture, hip fracture in first-degree relatives, comorbidities, and current medication use [26–28].

Dual-energy X-ray absorptiometry (DXA)

Areal bone mineral density (aBMD, g/cm^2) measurements of the lumbar spine (L1–L4) and proximal femur (femoral neck and total femur) were obtained by dual-energy X-ray absorptiometry (DXA) equipment (Hologic QDR 4500A; Hologic Inc. Bedford, MA, USA, Discovery model). All DXA measurements were performed by the same experienced technologist.

Precision error for DXA measurements was determined based on standard ISCD protocols [29]. We calculated the least significant change with 95% confidence to be 2.3% for the lumbar spine, 3.8% for the femoral neck, and 2.6% for the total femur.

Trabecular bone score (TBS) was calculated by the software TBS iNsight® version 2.1 (Med-Imaps, Bordeaux, France). It was analyzed as the mean value of the measurements for vertebrae L1–L4 of DXA images at exactly the same ROI as the spine BMD measurements. TBS values were classified according to the following criteria [10]: TBS $\geq$ 1.310: normal; 1.200 < TBS > 1.310: partially degraded

microarchitecture; TBS ≤ 1.200: degraded microarchitecture. In accordance with manufacturer recommendations, TBS was only assessed in patients with a BMI above 15 kg/m^2 and lower than 37 kg/m^2 [30].

High-resolution peripheral quantitative computed tomography (HR-pQCT)

The non-dominant radius and left tibia were immobilized on a carbon fiber shell and scanned on the first-generation HR-pQCT scanner (XtremeCT I, Scanco Medical AG, Brüttisellen, Switzerland) using a standard scanning protocol (60 kVp, 1000 µA). The measurements included 110 slices, corresponding to a 9.02 mm scan area (voxel size of 82 µm), positioned 9.5 mm and 22.5 mm proximal to the reference line for the distal radius and tibia, respectively.

All examinations were conducted by a trained biomedical scientist who also carefully examined each scan for motion artifacts. In the case of significant motion artifacts identified during scan acquisition, a second examination was performed. All HR-pQCT images were scored based on a motion scale ranging from 0 (no movement) to 4 (severe blurring of the periosteal surface and discontinuities in the cortical layer) [31, 32]. For the current study, scans with a score of 4 were excluded. Quality control was daily monitored using a phantom calibration provided by the manufacturer.

The standard morphologic analysis and advanced cortical (automated segmentation) method of the scanner were used for the analysis and have been described in detail elsewhere [20, 33, 34]. The outcome variables used in our analyses were density parameters, including total volumetric bone density (Tt.vBMD; mg HA/cm^3), trabecular volumetric bone density (Tb.vBMD; mg HA/cm^3), and cortical volumetric bone density (Ct.vBMD; mg HA/cm^3); structure parameters, including number (Tb.N; mm-1), thickness (Tb.Th; mm), and separation (Tb.Sp; mm) of trabeculae, cortical thickness (Ct.Th; mm), and cortical porosity (Ct.Po; %).

In our laboratory, HR-pQCT measurements in vivo had variation coefficients ranging from 1.49 to 7.59% at the distal radius and 0.78 to 6.35% at the distal tibia for morphometry parameters, and 0.93 to 1.41% at the distal radius and 0.25 to 1.16% at the distal tibia for densities [24, 33].

Finite element analysis (FEA)

To estimate bone strength from HR-pQCT measurements, linear finite element (FE) models of the distal radius and tibia were created directly from the HR-pQCT images using software-specific finite elements (Finite Element software v. 1.13, Scanco Medical AG, Switzerland, January 2009). The standard analysis of FEA comprises a virtual resistance test, which means that the computer analyzes the behavior of the bone tissue when it is submitted to a compressive force along its major axis. Two mechanical properties of the bone are estimated: Young's modulus, a measure of the ability of a material to return to its original shape after removal of a stress force, thus indicating the tissue's elasticity; and the Poisson effect, which is the tendency of a material to become thinner when it is stretched at a given axis. In other words, when a material is pulled, it increases its size in the axis of traction, and decreases its size in the other two axes. In response to the tensile force applied, the elasticity of the material will tend to bring it to its original shape. This trend can be understood as a force that will shrink the material in the direction of its stretching and will increase it in the other directions. The Poisson ratio is a ratio between the first and second forces [35].

The HR-pQCT images were filtered using a Laplace-Hamming filter and axial boundary conditions were assigned for compression tests with 1% strain (Young's modulus of 6829 MPa, Poisson's ratio of 0.3) [36].

Models of the distal radius and tibia were generated directly from the HR-pQCT images (Image Processing Language and FE Extension (IPLFE), Scanco Medical AG, Switzerland). The biomechanical properties studied were stiffness (S, kN/m) and failure load (F.Load, N).

Statistical analysis

Data were expressed as mean and standard deviation (SD), median and interquartile range (IQR), or number and percentage. To calculate the reference curves, multiple linear regression models were developed to predict the measurement of volumetric bone density, morphometry, and bone strength by FEA for distal radius and tibia as functions of age, weight, and height. Thus, the results of the microarchitecture parameters were illustrated using dispersion diagrams with their respective adjusted lines, using the mean of the height and weight measurements to estimate the models, as well as the respective 95% normality intervals. To evaluate the correlation between bone stiffness and other parameters obtained by HR-pQCT, Pearson's correlations were calculated.

We observed that the relationship with age, in some situations, did not show a linear relationship. Higher degree polynomials were tested and the quadratic relationship was sufficient in most non-linear models as a function of age. In this way, based on statistical analysis, a quadratic relationship was considered sufficient to adjust the models.

Statistical analyses were performed using IBM-SPSS software, version 20.0. P-values <0.05 were statistically significant.

Results

Reference curves according to the aging were developed including 340 men, of which 73% were Caucasian. Demographic, anthropometric, and clinical data are presented in Table 1. HR-pQCT measurements that showed movement artifacts were redone shortly after acquisition; thus, no participant was excluded after the analysis was completed. Representative 3D images of the distal radius and tibia for each age group are shown in Fig. 1.

Forty-seven (14 %) individuals reported previous fractures, all of them occurring after trauma. In the sites of fractures were radius, ulna, wrist, ankle, tibia, and fibula. No man had had experienced earlier vertebral fracture or fractures due to bone fragility. No comorbidity clinically relevant to the bone was reported by the participants.

DXA and TBS measurements are described in Table 1. All subjects had a BMI in the range of 18–35 kg/m^2 [median: 27 kg/m^2 (IQR: 25–29)], and no TBS adjustment was necessary. When stratified by TBS categories, 03 individuals aged 30–39 years, 05 aged 40–49 years, 07 aged 50–59 years, 08 aged 60–69 years, 28 aged 70–79 years, and 22 aged ≥ 80 years presented TBS <1.310.

Volumetric bone density, structure, cortical porosity, and bone strength estimated by FEA obtained by HR-pQCT as a function of age, weight, and height are described in Table 2 for the distal radius and tibia.

Multiple linear regression models were developed to predict the volumetric bone density, morphometry parameters, and estimated bone strength by FEA at the distal radius and tibia. These curves are illustrated using scatter plots (Figs. 2 and 3), which showed a linear relationship with age only for thickness measurements (trabecular and cortical) of distal radius and tibia (Fig. 2D, E), and bone strength at distal radius (Fig. 3A, B).

Table 3 shows that, at the distal region of the radius and tibia, all density and morphometry parameters had a statistically significant association with age but not with weight and height in men ($p < 0.05$). Pearson's correlations (r) between bone stiffness of peripheral regions with other variables measured by HR-pQCT at distal radius and tibia, areal BMD measures of the L1–L4 and left hip (femoral neck and total hip), and TBS are shown in Table 4.

At the distal radius site, except for some trabecular parameters (Tb.N and Tb.Sp) and for cortical porosity, the other variables showed a statistically significant correlation with stiffness (p <0.05), being positive (r> 0) or negative (r <0) correlations. At the distal tibial site, all parameters were statistically correlated with stiffness (p <0.05).

Table 1 Demographic and anthropometric characteristics, clinical data, and parameters of areal bone mineral density and trabecular bone score obtained by DXA of study population categorized by age

Variable	20–29 (n=50)	30–39 (n=51)	40–49 (n=46)	50–59 (n=51)	60–69 (n=50)	70–79 (n=50)	≥ 80 (n=42)
Age (years)	26 ± 2.8	34 ± 2.7	44 ± 3.1	55 ± 2.6	66 ± 2.1	76 ± 2.4	82 ± 3.1
Weight (kg)	79.4 ± 13.6	83.5 ± 11.5	81.4 ± 9.5	82.2 ± 12.4	78.9 ± 15.6	74.1 ± 12.2	69.8 ± 11.7
Height (cm)	1.75 ± 0.08	1.76 ± 0.07	1.73 ± 0.05	1.69 ± 0.08	1.66 ± 0.08	1.64 ± 0.07	1.61 ± 0.07
BMI (kg/m^2)	25.7 ± 3.3	26.8 ± 2.8	27.2 ± 2.7	28.7 ± 3.5	28.5 ± 4.8	27.5 ± 4.4	26.7 ± 2.9
Race (n [%])							
Caucasian	37 (74)	40 (78)	32 (70)	38 (74)	34 (68)	40 (80)	28 (67)
Other races	13 (26)	11 (22)	14 (30)	13 (26)	16 (32)	10 (20)	14 (33)
Arterial hypertension (n [%])	0	0	0	2 (4)	8 (16)	6 (12)	1 (2)
BMD L1–L4 (g/cm^2)	1.097 (1.019; 1.219)	1.042 (0.974; 1.163)	1.011 (0.901; 1.125)	1.030 (0.973; 1.129)	1.033 (0.888; 1.235)	1.113 (0.953; 1.225)	1.095 (0.912; 1.275)
BMD femoral neck (g/cm^2)	1.035 (0.901; 1.162)	0.938 (0.852; 0.985)	0.891 (0.791; 0.993)	0.820 (0.737; 0.957)	0.793 (0.717; 0.851)	0.805 (0.673; 0.890)	0.762 (0.641; 0.803)
BMD total hip (g/cm^2)	1.084 (0.978; 1.233)	1.071 (0.976; 1.142)	1.009 (0.940; 1.109)	1.015 (0.946; 1.099)	1.042 (0.901; 1.140)	0.979 (0.866; 1.078)	0.938 (0.834; 1.067)
TBS	1.480 (1.439; 1.536)	1.432 (1.376; 1.489)	1.374 (1.336; 1.447)	1.381 (1.338; 1.424)	1.381 (1.314; 1.440)	1.291 (1.217; 1.348)	1.300 (1.244; 1.380)

Data are shown as mean ± SD, number (percentage), or median (interquartile interval)

BMI body mass index; *BMD* bone mineral density; *TBS* trabecular bone score

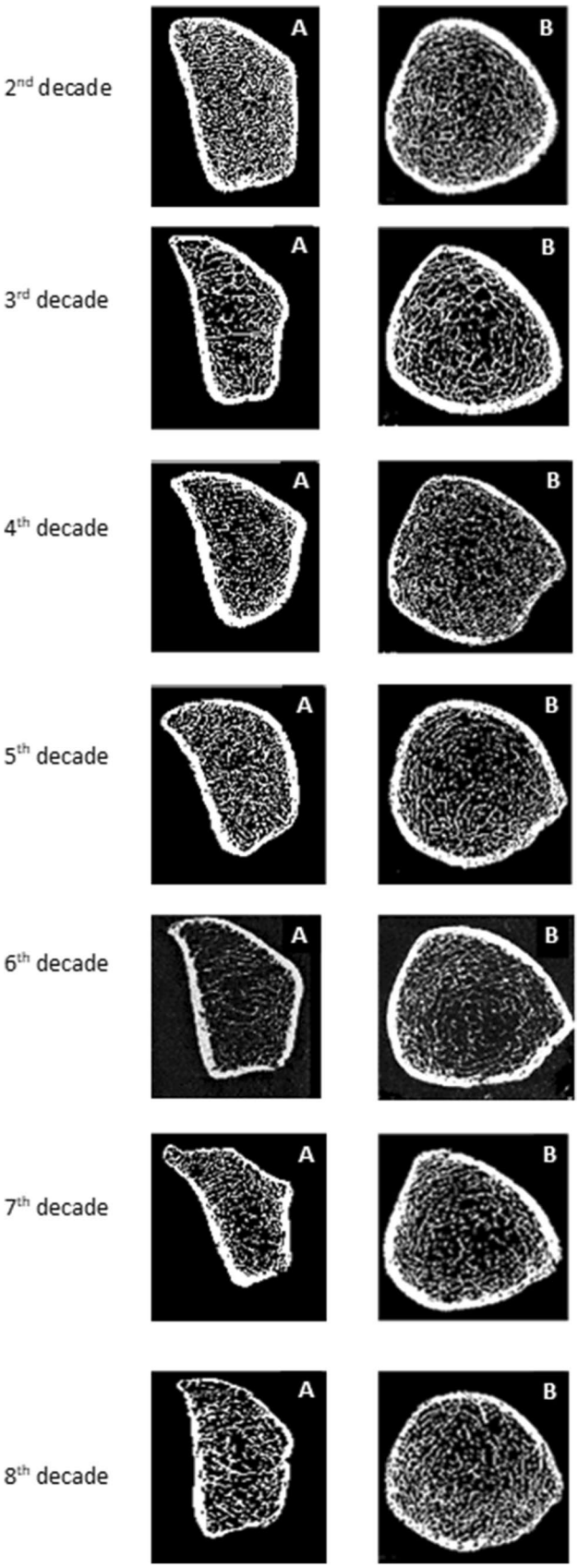

Fig. 1 3D images of the left distal radius (A) and left distal tibia (B) for each age group

Discussion

This study provides HR-pQCT reference data for a selected population of healthy men in Brazil and demonstrates that age, weight, and height are associated to changes in bone mass and microstructural properties which behave differently in the cortical and trabecular compartments of both distal radius and tibia.

An interesting feature of the current study is the weight and height adjustments of the bone parameters in addition to age adjustments. Speculatively, significant changes occurring in weight and height with aging may lead to an increased ratio of body fat which may affect bone metabolism and bone loss. Also, the gender restriction (only male population) is clinically useful given that risk factors for osteoporosis and fractures are different in men and women [5, 7, 20].

Concerning to the clinical applicability of HR-pQCT, the implementation of age- and sex-specific reference data in different populations is limited. In the current study, we developed reference values for volumetric bone density and morphometry parameters from HR-pQCT, and bone strength estimated by finite element, at the distal sites of the radius and tibia, categorized by decades, for a healthy male sample representing a main part of the Brazilian miscegenated population.

Different from DXA, to determine T-scores for the HR-pQCT data is difficult because of the great variety of existing parameters, which show distinct behaviors throughout life [8]. In addition, there are differences in the aging bone changes between the regions of radius and tibia [16, 24, 37].

In this HR-pQCT study, almost half of the statistical models had a quadratic relationship with age, and all parameters had a statistically significant association with age in men. Density and trabecular microarchitecture changes in the advanced age might be related to local trabecularization of the cortical bone [38]. The cortical porosity increased with age, mainly at the tibia site. According to Burt et al. [16], in adulthood, cortical porosity increases as bone resorption exceeds formation over the years. It suggests that this variable could be clinically relevant for the stratification of fracture risk and the classification of diseases such as osteoporosis [16].

In FEA, bone stiffness at the tibia had a greater correlation with other HR-pQCT and DXA parameters than at the radius. These results may be related to differences in weight-bearing capacities between the two sites [39].

Furthermore, bone stiffness was correlated to the cortical bone compartment in both analyzed regions. According to the literature, cortical vBMD influences bone capacity to absorb energy during the bone mechanical overload

Table 2 Reference values of bone geometry, volumetric bone density, structure, cortical porosity and bone strength estimated by finite element obtained by HR-pQCT at distal radius and tibia of 340 healthy men from 20 to 92 years old, expressed as median and interquartile interval

Variable	20–29 (n=50)	30–39 (n=51)	40–49 (n=46)	50–59 (n=51)	60–69 (n=50)	70–79 (n=50)	≥ 80 (n=42)
	Median (IQR)	Median (IQR)	Median (IQR)	Median (IQR)	Median (IQR)	Median (IQR)	Median (IQR)
Radius							
Tt.vBMD (mg HA/cm^3)	358.0 (331.4; 409.3)	350.7 (304.1; 396.4)	348.7 (305.7; 397.1)	332.8 (286.5; 376.9)	298.3 (269.3; 346.8)	303.3 (261.7; 368.6)	298.0 (258.6; 337.2)
Tb.vBMD (mg HA/cm^3)	217.5 (200.3; 241.4)	211.3 (182.4; 240.8)	190.1 (164.1; 223.4)	180.7 (165.0; 195.4)	180.3 (148.2; 195.6)	181.5 (154.2; 216.3)	187.4 (172.2; 199.7)
Ct.vBMD (mg HA/cm^3)	990.8 (945.8; 1014.4)	985.1 (954.2; 1006.7)	1001.3 (939.5; 1038.1)	954.9 (910.6; 1001.9)	941.5 (916.5; 979.7)	931.5 (899.6; 968.3)	903.7 (856.4; 950.6)
Tb.N (1/mm)	2.26 (2.01; 2.36)	2.24 (2.03; 2.39)	2.08 (1.72; 2.33)	2.11 (1.99; 2.25)	2.08 (1.82; 2.30)	2.14 (1.90; 2.35)	2.10 (1.91; 2.28)
Tb.Th (mm)	0.082 (0.077; 0.091)	0.079 (0.071; 0.086)	0.080 (0.066; 0.091)	0.073 (0.066; 0.080)	0.070 (0.066; 0.082)	0.073 (0.066; 0.079)	0.072 (0.067; 0.078)
Tb.Sp (mm)	0.356 (0.340; 0.418)	0.366 (0.340; 0.414)	0.413 (0.358; 0.468)	0.402 (0.378; 0.436)	0.408 (0.373; 0.471)	0.389 (0.354; 0.457)	0.399 (0.365; 0.445)
Ct.Th (mm)	0.981 (0.902; 1.074)	0.907 (0.792; 1.063)	0.991 (0.879; 1.145)	0.961 (0.837; 1.153)	0.864 (0.761; 0.945)	0.899 (0.756; 1.045)	0.824 (0.684; 0.900)
Ct.Po (%)	2.01 (1.51; 2.84)	1.94 (1.60; 2.53)	1.96 (1.67; 2.22)	2.63 (2.04; 3.26)	2.44 (2.10; 3.29)	3.82 (2.75; 4.94)	3.65 (3.14; 5.10)
S (kN/m)	115,461 (103,467; 135,535)	117,898 (106,225; 127,617)	114,086 (103,868; 141,448)	100,902 (93,960; 122,214)	94,317 (88,916; 109,564)	100,394 (81,594; 116,161)	96,992 (88,376; 108,084)
F.Load (N)	5595 (5025; 6637)	5665 (5133; 6232)	5337 (4975; 6709)	4878 (4592; 5949)	5185 (4341; 7000)	4944 (4058; 5973)	4754 (4250; 5318)
Tibia							
Tt.vBMD (mg HA/cm^3)	345.9 (331.2; 381.9)	323.0 (300.4; 370.9)	305.4 (253.1; 329.5)	296.8 (282.3; 351.2)	281.3 (254.5; 318.3)	291.7 (248.9; 322.7)	280.2 (258.5; 323.1)
Tb.vBMD (mg HA/cm^3)	218.5 (199.3; 244.4)	198.3 (179.3; 223.5)	166.0 (134.2; 194.1)	169.7 (156.1; 195.8)	158.3 (149.2; 186.7)	169.6 (140.8; 187.3)	157.7 (144.4; 186.1)
Ct.vBMD (mg HA/cm^3)	951.5 (929.3; 991.7)	975.4 (945.9; 997.0)	957.7 (923.5; 995.8)	917.7 (901.8; 952.4)	913.0 (888.7; 952.2)	890.9 (837.8; 932.8)	863.2 (824.3; 900.5)
Tb.N (1/mm)	2.18 (1.97; 2.42)	2.11 (1.88; 2.27)	1.85 (1.55; 2.14)	1.82 (1.71; 2.23)	1.76 (1.62; 2.11)	1.91 (1.60; 2.14)	1.86 (1.61; 2.04)
Tb.Th (mm)	0.084 (0.072; 0.090)	0.078 (0.068; 0.096)	0.074 (0.064; 0.082)	0.075 (0.069; 0.079)	0.078 (0.071; 0.083)	0.074 (0.063; 0.087)	0.076 (0.067; 0.080)
Tb.Sp (mm)	0.381 (0.328; 0.430)	0.391 (0.366; 0.433)	0.481 (0.391; 0.555)	0.451 (0.376; 0.516)	0.488 (0.397; 0.544)	0.447 (0.396; 0.539)	0.464 (0.418; 0.555)
Ct.Th (mm)	1.470 (1.260; 1.620)	1.412 (1.233; 1.546)	1.338 (1.140; 1.469)	1.357 (1.138; 1.526)	1.253 (1.140; 1.397)	1.321 (1.100; 1.425)	1.243 (1.113; 1.350)
Ct.Po (%)	4.32 (3.23; 5.62)	4.88 (3.55; 5.66)	4.32 (3.68; 6.43)	5.45 (4.67; 6.72)	7.21 (5.24; 8.88)	7.61 (5.86; 9.39)	8.97 (8.14; 10.27)
S (kN/m)	330,819 (282,292; 349,819)	297,542 (276,074; 335,006)	276,731 (248,341; 323,281)	254,900 (227,805; 290,378)	242,488 (210,642; 280,251)	246,891 (218,414; 274,239)	214,418 (202,105; 252,780)
F.Load (N)	16,331 (14,482; 17,778)	14,387 (13,315; 16,024)	13,188 (11,757; 15,062)	12,280 (10,800; 14,099)	12,195 (10,209; 13,453)	11,919 (10,424; 13,250)	9965 (9155; 11,802)

Data are shown as median (IQR: interquartile interval)

Ct.Pm cortical perimeter; *Ct.Ar* cortical area; *Tb.Ar* trabecular area; *Tt.vBMD* total volumetric bone density; *Tb.vBMD* trabecular volumetric bone density; *Ct.vBMD* cortical volumetric bone density; *Tb.N* number of trabeculae; *Tb.Th* trabecular thickness; *Tb.Sp* trabecular separation; *Ct.Th* cortical thickness; *Ct.Po* cortical porosity; *S* stiffness; *F.Load* failure load

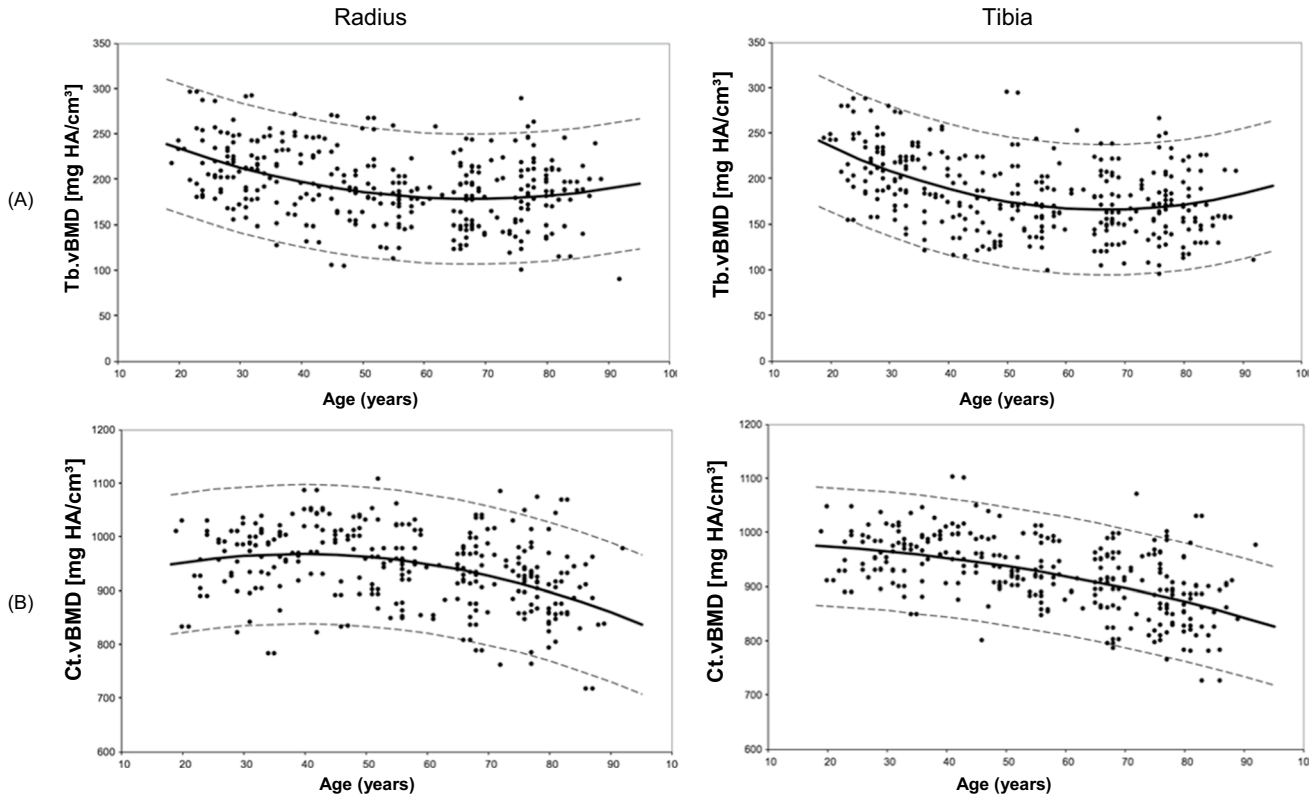

Fig. 2 Reference curves depending on the age of a volumetric bone density, structure, and cortical porosity parameters, being (A) trabecular volumetric bone density (Tb.vBMD), (B) cortical volumetric bone density (Ct.vBMD), (C) number of trabeculae (Tb.N), (D) trabecular thickness (Tb.Th), (E) cortical thickness (Ct.Th), (F) cortical porosity (Ct.Po) obtained by HR-pQCT in the radius region (left) and tibia (right) in healthy men distributed by age groups. The solid line represents the mean from the regression model, and dashed lines represent the confidence interval of 95% prevision

process and is likely to be an important determinant of fracture risk [40]. Moreover, consistent with previous reports, bone stiffness was significantly correlated with areal BMD, especially at the femoral neck [41].

Bone stiffness was also correlated with trabecular volumetric bone density and trabecular structural parameters by HR-pQCT and TBS. Of note, the trabecular compartment is crucial to bone strength. As demonstrated by Burrows et al. [42], the number of trabeculae is significantly higher for men than women in all age groups, suggesting that a larger trabecular structure would increase bone stiffness and consequently improve fracture resistance. In fact, according to a recent study from our group, men had more trabeculae than women in all age groups, as well bone strength parameters estimated by finite element were higher for men compared to women [43].

Thus, a weak to moderate correlation between stiffness and density/structural parameters was detected in both compartments and at both peripheral sites, suggesting that bone strength is dependent on both trabecular and cortical bone. Although the magnitude of the correlation between FEA and most bone microstructural parameters provided by HR-pQCT is low, it helps to determine the contribution of each of these variables to fracture risk prediction, given that FEA provides an estimate of bone strength. Our data are consistent with the literature, which shows that both the cortical and trabecular bones contribute to the predicted failure load [44].

Although approximately 70% of our cohort was considered Caucasian, Brazil has very large with substantial ethnic admixture and distinct lifestyle habits, configuring a miscegenated population [25]. It is different from the Caucasian population of North America and Europe, for example. It is known that there are ethnic differences in the skeletal parameters [45, 46]. Thus, reference data reported in this study may be more adequate for miscegenated populations.

Potential limitations of this study include degenerative changes in the lumbar spine such as osteophytes and aortic

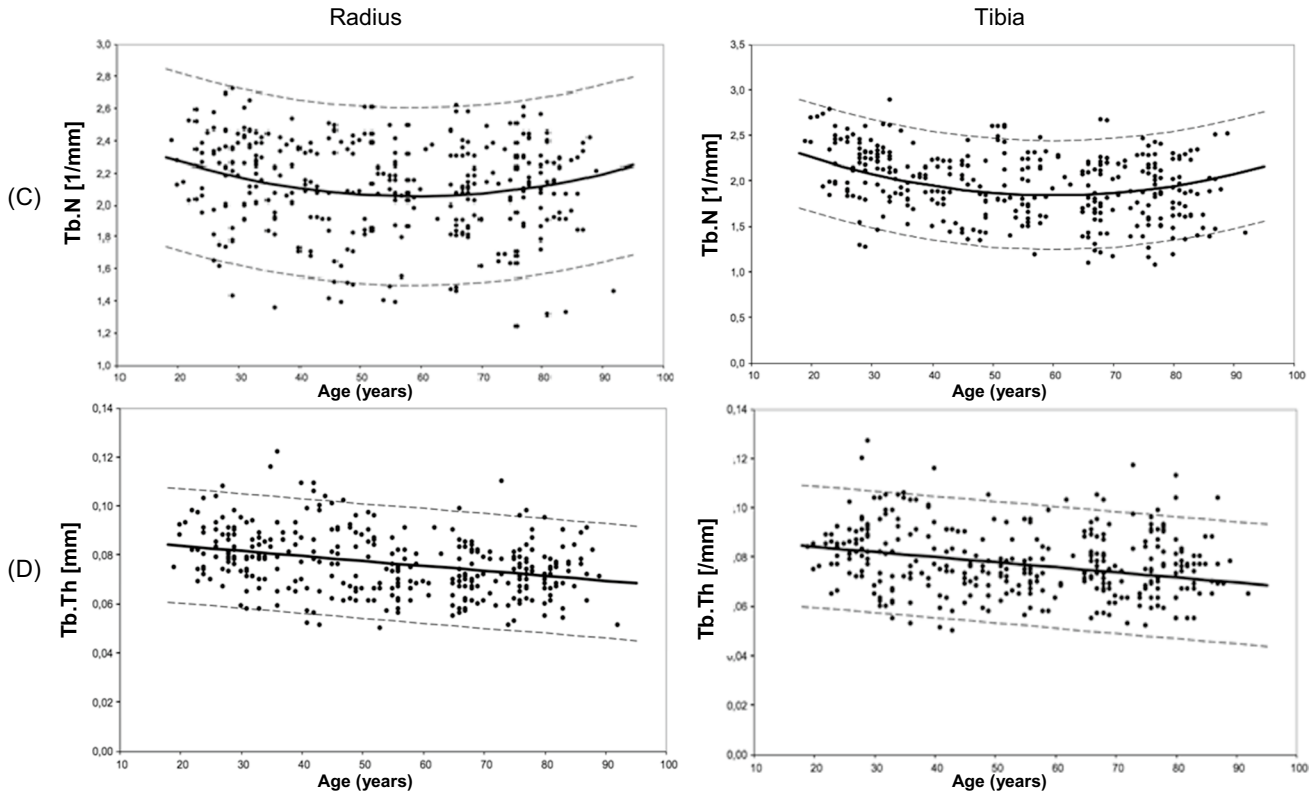

Fig. 2 (continued)

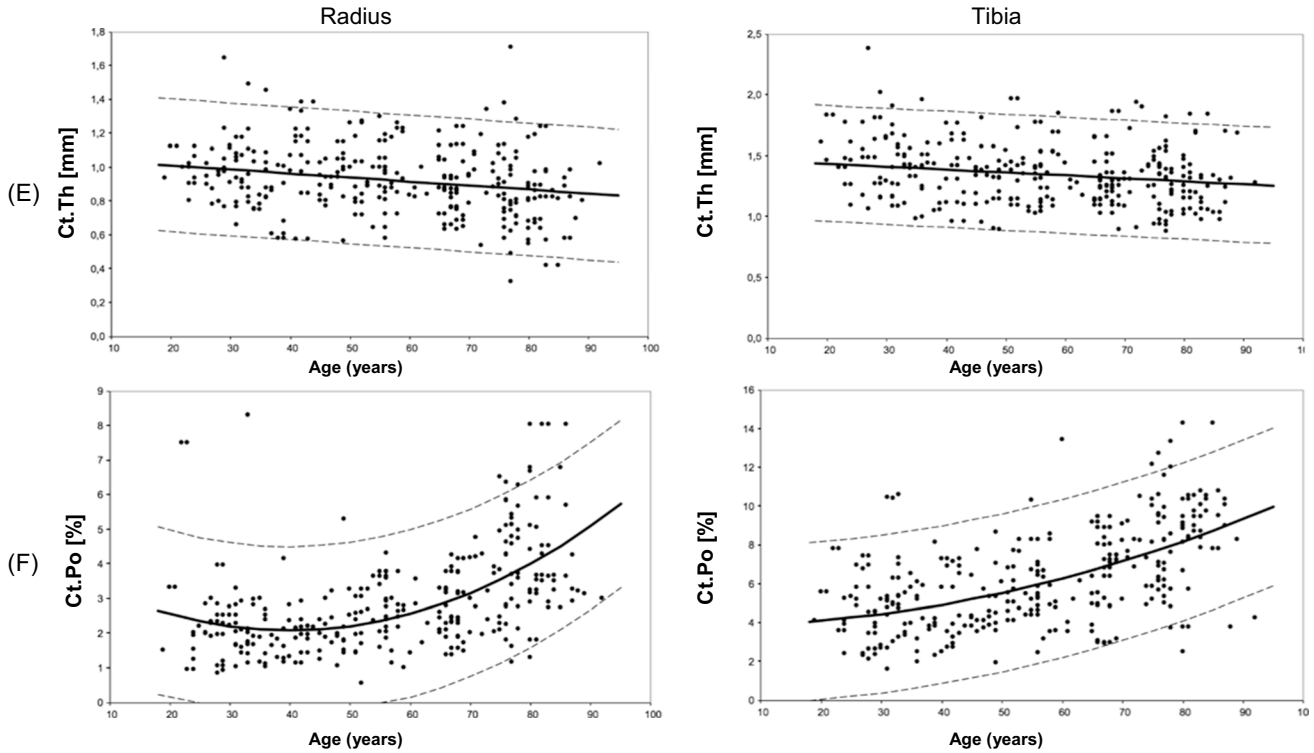

Fig. 2 (continued)

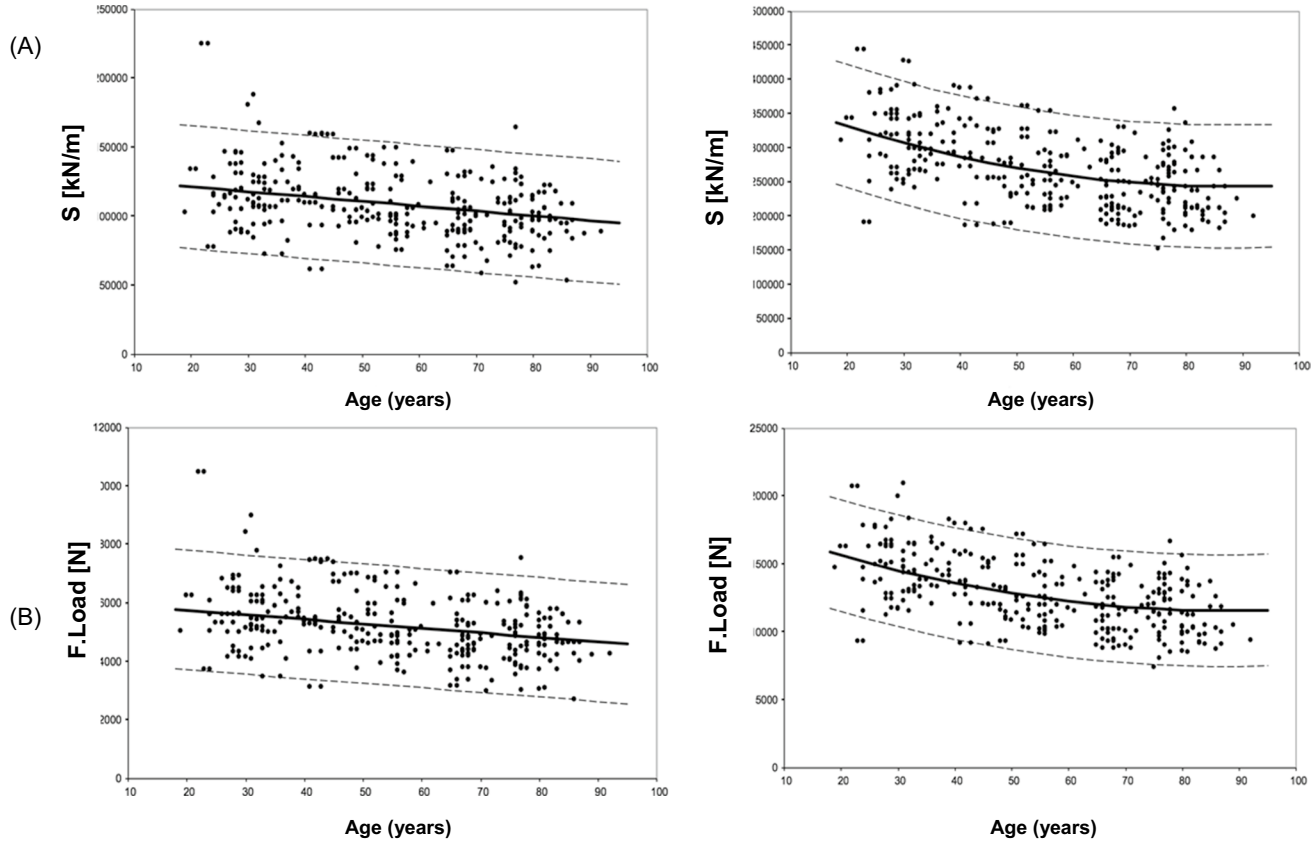

Fig. 3 Reference curves depending on the age of the bone strength parameters estimated by finite element, being (A) stiffness (S) and (B) failure load (F.Load) obtained by HR-pQCT in the radius region (left) and tibia (right) in healthy men distributed by age groups. The solid line represents the mean from the regression model, and dashed lines represent the confidence interval of 95% prevision

calcification that may have overestimated areal BMD (DXA). Besides this, the sample consisted of a healthy population that included individuals with osteopenia and osteoporosis, resulting in a broad spectrum of areal BMD. Moreover, it was not possible to separate participants into racial groups because of the larger number of Caucasian individuals than other races. The oldest participant in our study was 92 years old. Due to the limited number of participants aged 90 years or older in our cohort, there was no statistical ability to generate reference results over this decade.

In conclusion, the current study expands the HR-pQCT worldwide database. As this is a specific selected sample, the results may not be directly extrapolable to other male populations. Anyway, the study brings an adequate methodology for the construction of reference data in other populations. We hope it can stimulate longitudinal research on HR-pQCT.

Table 3 Multiple linear regression analysis to explain the bone microarchitecture parameters obtained by HR-pQCT at distal radius and tibia of 340 healthy men according to the age, weight, and height

Variable	Factor	Coefficient	Standard error	*t* value	*p*	R^2
Radius						
Tb.vBMD (mg HA/cm^3)	Constant	276.95	58.53	4.73	**<0.001**	0.150
	Age (years)	−3.27	0.69	−4.71	**<0.001**	
	Height (cm)	−0.14	33.96	0.00	0.997	
	Weight (kg)	0.165	0.192	0.86	0.389	
	Age^2 (years^2)	0.024	0.006	3.87	**<0.001**	
Ct.vBMD (mg HA/cm^3)	Constant	921.44	114.20	8.07	**<0.001**	0.152
	Age (years)	3.30	1.35	2.45	**0.015**	
	Height (cm)	37.60	65.35	0.58	0.566	
	Weight (kg)	−1.04	0.36	−2.88	**0.004**	
	Age^2 (years^2)	−0.04	0.01	−3.46	**0.001**	
Tb.N (1/mm)	Constant	2.26	0.45	4.99	**<0.001**	0.072
	Age (years)	−0.017	0.005	−3.20	**0.001**	
	Height (cm)	−0.025	0.262	−0.10	0.923	
	Weight (kg)	0.0044	0.0015	2.95	**0.003**	
	Age^2 (years^2)	0.00015	0.00005	2.99	**0.003**	
Tb.Th (mm)	Constant	0.087	0.018	4.73	**<0.001**	0.108
	Age (years)	−0.00020	0.00004	−4.79	**<0.001**	
	Height (cm)	0.00578	0.01112	0.52	0.604	
	Weight (kg)	−0.00011	0.00006	−1.83	0.068	
Ct.Th (mm)	Constant	0.864	0.329	2.63	**0.009**	0.062
	Age (years)	−0.0024	0.0008	−3.11	**0.002**	
	Height (cm)	0.149	0.198	0.75	0.452	
	Weight (kg)	−0.0007	0.0011	−0.67	0.503	
Ct.Po (%)	Constant	2.66	1.97	1.35	0.178	0.283
	Age (years)	−0.10	0.03	−3.79	**<0.001**	
	Height (cm)	0.77	1.17	0.66	0.513	
	Weight (kg)	0.0004	0.0068	0.06	0.950	
	Age^2 (years^2)	0.0012	0.0002	5.31	**<0.001**	
S (kN/m)	Constant	48857.6	35012.7	1.40	0.164	0.158
	Age (years)	−344.5	82.4	−4.18	**<0.001**	
	Height (cm)	42116.5	21461.4	1.96	0.051	
	Weight (kg)	95.1	121.1	0.79	0.433	
F.Load (N)	Constant	2381.9	1602.2	1.49	0.138	0.157
	Age (years)	−15.5	3.8	−4.11	**<0.001**	
	Height (cm)	1957.6	982.1	1.99	**0.047**	
	Weight (kg)	4.5	5.5	0.82	0.414	
Tibia						
Tb.vBMD (mg HA/cm^3)	Constant	298.30	58.88	5.07	**<0.001**	0.239
	Age (years)	−4.26	0.70	−6.12	**<0.001**	
	Height (cm)	−14.33	34.08	−0.42	0.674	
	Weight (kg)	0.427	0.192	2.22	**0.027**	
	Age^2 (years^2)	0.032	0.006	5.01	**<0.001**	
Ct.vBMD (mg HA/cm^3)	Constant	990.51	87.19	11.36	**<0.001**	0.281
	Height (cm)	19.32	54.36	0.36	0.723	
	Weight (kg)	−0.54	0.30	−1.79	0.074	
	Age^2 (years^2)	−0.017	0.002	−8.74	**<0.001**	
Tb.N (1/mm)	Constant	1.30	0.49	2.64	**0.009**	0.297
	Age (years)	−0.031	0.006	−5.34	**<0.001**	
	Height (cm)	0.392	0.284	1.38	0.169	
	Weight (kg)	0.0103	0.0016	6.45	**<0.001**	
	Age^2 (years^2)	0.00026	0.00005	4.89	**<0.001**	
Tb.Th (mm)	Constant	0.131	0.019	6.76	**<0.001**	0.109
	Age (years)	−0.00021	0.00005	−4.63	**<0.001**	
	Height (cm)	−0.014	0.012	−1.16	0.245	
	Weight (kg)	−0.00024	0.00007	−3.63	**<0.001**	

Table 3 (continued)

Variable	Factor	Coefficient	Standard error	*t* value	*p*	R^2
Ct.Th (mm)	Constant	1.03	0.40	2.56	**0.011**	0.063
	Age (years)	−0.0024	0.0009	−2.60	**0.010**	
	Height (cm)	0.281	0.241	1.17	0.245	
	Weight (kg)	−0.0003	0.0013	−0.20	0.843	
Ct.Po (%)	Constant	2.30	3.08	0.75	0.455	0.319
	Height (cm)	0.56	1.96	0.29	0.774	
	Weight (kg)	0.0074	0.0110	0.67	0.507	
	Age^2 (years^2)	0.0007	0.0001	10.13	**<0.001**	
S (kN/m)	Constant	199915.0	73419.5	2.72	**0.007**	0.329
	Age (years)	−3388.5	933.1	−3.63	**<0.001**	
	Height (cm)	104612.7	43207.6	2.42	**0.016**	
	Weight (kg)	175.5	246.8	0.71	0.478	
	Age^2 (years^2)	19.4	8.4	2.30	**0.022**	
F.Load (N)	Constant	8819.3	3348.4	2.63	**0.009**	0.341
	Age (years)	−153.7	42.6	−3.61	**<0.001**	
	Height (cm)	5184.4	1970.6	2.63	**0.009**	
	Weight (kg)	9.03	11.26	0.80	0.423	
	Age^2 (years^2)	0.87	0.39	2.26	**0.024**	

*Adjusted for age, weight, and height; bold = p <0.05

R^2: coefficient of determination

Tb.vBMD trabecular volumetric bone density; *Ct.vBMD* cortical volumetric bone density; *Tb.N* number of trabeculae; *Tb.Th* trabecular thickness; *Ct.Th* cortical thickness; *Ct.Po* cortical porosity; *S* stiffness; *F.Load* failure load

Table 4 Pearson's correlation between bone stiffness parameter estimated by finite element analysis with bone parameters obtained by distal radius and tibia HR-pQCT scan, and areal BMD and TBS parameters obtained by DXA in 340 healthy men

Variable	Radius		Tibia	
	r	*p*	*r*	*p*
Tt.vBMD (mg HA/cm^3)	0.253	**<0.001**	0.378	**<0.001**
Tb.vBMD (mg HA/cm^3)	0.282	**<0.001**	0.423	**<0.001**
Ct.vBMD (mg HA/cm^3)	0.213	**<0.001**	0.337	**<0.001**
Tb.N (1/mm)	0.056	0.325	0.357	**<0.001**
Tb.Th (mm)	0.301	**<0.001**	0.181	**0.001**
Tb.Sp (mm)	−0.079	0.162	−0.347	**<0.001**
Ct.Th (mm)	0.279	**<0.001**	0.355	**<0.001**
Ct.Po (%)	−0.011	0.843	−0.296	**<0.001**
F.Load (N)	0.997	**<0.001**	0.997	**<0.001**
BMD L1–L4 (g/cm^2)	0.164	**0.004**	0.213	**<0.001**
BMD femoral neck (g/cm^2)	0.326	**<0.001**	0.477	**<0.001**
BMD total hip (g/cm^2)	0.237	**<0.001**	0.391	**<0.001**
TBS	0.317	**<0.001**	0.429	**<0.001**

Ct.Pm cortical perimeter; *Ct.Ar* cortical area; *Tb.Ar* trabecular area; *Tt.vBMD* total volumetric bone density; *Tb.vBMD* trabecular volumetric bone density; *Ct.vBMD* cortical volumetric bone density; *Tb.N* number of trabeculae; *Tb.Th* trabecular thickness; *Tb.Sp* trabecular separation; *Ct.Th* cortical thickness; *Ct.Po* cortical porosity; *F.Load* failure load; *BMD* bone mineral density; *TBS* trabecular bone score

Acknowledgements The authors thank Steven Boyd, PhD for research support. We further cordially thank Rogerio Ruscitto, PhD for statistical analysis.

Funding This work was supported by Fundação de Amparo à Pesquisa do Estado de São Paulo (FAPESP) #2017/00693-7 (JCA); #2015/14698-5 (JCA) and Conselho Nacional de Ciência e Tecnologia (CNPq) #305556/2017-7 (RMRP).

Declarations

Conflicts of interest None.

References

1. Delaisse JM (2014) The reversal phase of the bone-remodeling cycle: cellular prerequisites for coupling resorption and formation. Bonekey Rep 6(3):561
2. National Osteoporosis Foundation (2002) America's Bone Health: The State of Osteoporosis and Low Bone Mass in Our Nation. National Osteoporosis Foundation, Washington
3. Gullberg B, Johnell O, Kanis JA (1997) World-wide projections for hip fracture. Osteoporos Int 7(5):407–413
4. Bliuc D, Nguyen ND, Milch VE, Nguyen TV, Eisman JA, Center JR (2009) Mortality risk associated with low-trauma osteoporotic fracture and subsequent fracture in men and women. JAMA 301:513–521

5. Melton LJ (1995) Epidemiology of fractures. In: Riggs BL, Melton LJ (eds) Osteoporosis: etiology, diagnosis and management, 2nd edn. Lipponcott-Raven, Philadelphia
6. Merrill RM, Weed DL, Feuer EJ (1997) The lifetime risk of developing prostate cancer in white and black men. Cancer Epidemiol Biomarkers Prev: a publication of the American Association for Cancer Research, cosponsored by the American Society of Preventive Oncology 6:763–768
7. Schuit SC, van der Klift M, Weel AE, de Laet CE, Burger H, Seeman E, Hofman A, Uitterlinden AG, van Leeuwen JP, Pols HA (2004) Fracture incidence and association with bone mineral density in elderly men and women: the Rotterdam Study. Bone 34(1):195–202
8. Burt LA, Liang Z, Sajobi TT, Hanley DA, Boyd SK (2016) Sex- and site-specific normative data curves for HR-pQCT. J Bone Miner Res 31(11):2041–2047
9. Stein EM, Kepley A, Walker M, Nickolas TL, Nishiyama K, Zhou B, Liu XS, McMahon DJ, Zhang C, Boutroy S, Cosman F, Nieves J, Guo XE, Shane E (2014) Skeletal structure in postmenopausal women with osteopenia and fractures is characterized by abnormal trabecular plates and cortical thinning. J Bone Miner Res 29(5):1101–1109
10. McCloskey EV, Odén A, Harvey NC, Leslie WD, Hans D, Johansson H, Barkmann R, Boutroy S, Brown J, Chapurlat R, Elders PJM, Fujita Y, Glüer CC, Goltzman D, Iki M, Karlsson M, Kindmark A, Kotowicz M, Kurumatani N et al (2016) A meta-analysis of trabecular bone score in fracture risk prediction and its relationship to FRAX. J Bone Miner Res 31(5):940–948
11. Hans D, Goertzen AL, Krieg MA, Leslie WD (2011) Bone microarchitecture assessed by TBS predicts osteoporotic fractures independent of bone density: the Manitoba study. J Bone Miner Res 26(11):2762–2769
12. Schousboe JT, Vo T, Taylor BC, Cawthon PM, Schwartz AV, Bauer DC, Orwoll ES, Lane NE, Barrett-Connor E, Ensrud KE (2016) Osteoporotic Fractures in Men MrOS Study Research Group. Prediction of incident major osteoporotic and hip fractures by trabecular bone score (TBS) and prevalent radiographic vertebral fracture in older men. J Bone Miner Res 31(3):690–697
13. Patsch JM, Burghardt AJ, Kazakia G, Majumdar S (2011) Noninvasive imaging of bone microarchitecture. Ann N Y Acad Sci 1240:77–87
14. Vilayphiou N, Boutroy S, Sornay-Rendu E, Van Rietbergen B, Munoz F, Delmas PD, Chapurlat R (2010) Finite element analysis performed on radius and tibia HR-pQCT images and fragility fractures at all sites in postmenopausal women. Bone 46(4):1030–1037
15. Liu XS, Zhang XH, Sekhon KK, Adams MF, McMahon DJ, Bilezikian JP, Shane E, Guo XE (2010) High-resolution peripheral quantitative computed tomography can assess microstructural and mechanical properties of human distal tibial bone. J Bone Miner Res 25(4):746–756
16. Burt LA, Macdonald HM, Hanley DA, Boyd SK (2014) Bone microarchitecture and strength of the radius and tibia in a reference population of young adults: an HR-pQCT study. Arch Osteoporos 9:183
17. Fuller H, Fuller R, Pereira RM (2015) High resolution peripheral quantitative computed tomography for the assessment of morphological and mechanical bone parameters. Rev Bras Reumatol 55(4):352–362
18. Vilayphiou N, Boutroy S, Sornay-Rendu E, Van Rietbergen B, Chapurlat R (2016) Age-related changes in bone strength from HR-pQCT derived microarchitectural parameters with an emphasis on the role of cortical porosity. Bone 83:233–240
19. Burghardt AJ, Kazakia GJ, Ramachandran S, Link TM, Majumdar S (2010) Age- and gender-related differences in the geometric properties and biomechanical significance of intracortical porosity in the distal radius and tibia. J Bone Miner Res 25(5):983–993
20. Macdonald HM, Nishiyama KK, Kang J, Hanley DA, Boyd SK (2011) Age-related patterns of trabecular and cortical bone loss differ between sexes and skeletal sites: a population-based HR-pQCT study. J Bone Miner Res 26(1):50–62
21. Khosla S, Riggs BL, Atkinson EJ, Oberg AL, McDaniel LJ, Holets M, Peterson JM, Melton LJ (2006) 3rd. Effects of sex and age on bone microstructure at the ultradistal radius: a population-based noninvasive in vivo assessment. J Bone Miner Res 21(1):124–131
22. Amin S, Khosla S (2012) Sex- and age-related differences in bone microarchitecture in men relative to women assessed by high-resolution peripheral quantitative computed tomography. J Osteoporos 2012:129760
23. Hansen S, Shanbhogue V, Folkestad L, Nielsen MM, Brixen K (2014) Bone microarchitecture and estimated strength in 499 adult Danish women and men: a cross-sectional, population-based high-resolution peripheral quantitative computed tomographic study on peak bone structure. Calcif Tissue Int 94(3):269–281
24. Alvarenga JC, Fuller H, Pasoto SG, Pereira RM (2017) Age-related reference curves of volumetric bone density, structure, and biomechanical parameters adjusted for weight and height in a population of healthy women: an HR-pQCT study. Osteoporos Int 28(4):1335–1346
25. Fuchs SC, Guimarães SM, Sortica C, Wainberg F, Dias KO, Ughini M, Castro JA, Fuchs FD (2002) Reliability of race assessment based on the race of the ascendants: a cross-sectional study. BMC Public Health 2:1
26. Lopes JB, Fung LK, Cha CC, Gabriel GM, Takayama L, Figueiredo CP, Pereira RM (2012) The impact of asymptomatic vertebral fractures on quality of life in older community-dwelling women: the São Paulo Ageing & Health Study. Clinics (Sao Paulo) 67(12):1401–1406
27. Bhalla AK (2010) Management of osteoporosis in a pre-menopausal woman. Best Pract Res Clin Rheumatol 24(3):313–327
28. Eviö S, Tiitinen A, Laitinen K, Ylikorkala O, Välimäki MJ (2004) Effects of alendronate and hormone replacement therapy, alone and in combination, on bone mass and markers of bone turnover in elderly women with osteoporosis. J Clin Endocrinol Metab 89(2):626–631
29. Shuhart CR, Yeap SS, Anderson PA, Jankowski LG, Lewiecki EM, Morse LR, Rosen HN, Weber DR, Zemel BS, Shepherd JA (2019) Executive Summary of the 2019 ISCD position development conference on monitoring treatment, DXA cross-calibration and least significant change, spinal cord injury, periprosthetic and orthopedic bone health, transgender medicine, and pediatrics. J Clin Densitom 22(4):453–471
30. Silva BC, Broy SB, Boutroy S, Schousboe JT, Shepherd JA, Leslie WD (2015) Fracture risk prediction by non-BMD DXA measures: the 2015 ISCD official positions part 2: trabecular bone score. J Clin Densitom 18(3):309–330
31. Paggiosi MA, Eastell R, Walsh JS (2014) Precision of high-resolution peripheral quantitative computed tomography measurement variables: influence of gender, examination site, and age. Calcif Tissue Int 94(2):191–201
32. Pauchard Y, Liphardt AM, Macdonald HM, Hanley DA, Boyd SK (2012) Quality control for bone quality parameters affected by subject motion in high-resolution peripheral quantitative computed tomography. Bone 50(6):1304–1310
33. Paupitz JA, Lima GL, Alvarenga JC, Oliveira RM, Bonfa E, Pereira RM (2016) Bone impairment assessed by HR-pQCT in juvenile-onset systemic lupus erythematosus. Osteoporos Int 27(5):1839–1848
34. Buie HR, Campbell GM, Klinck RJ, MacNeil JA, Boyd SK (2007) Automatic segmentation of cortical and trabecular compartments based on a dual threshold technique for in vivo micro-CT bone analysis. Bone 41(4):505–515

35. Sundar SS, Nandlal B, Saikrishna D, Mallesh G (2012) Finite element analysis: a maxillofacial surgeon's perspective. J Maxillofac Oral Surg 11(2):206–211
36. Macneil JA, Boyd SK (2008) Bone strength at the distal radius can be estimated from high-resolution peripheral quantitative computed tomography and the finite element method. Bone 42(6):1203–1213. https://doi.org/10.1016/j.bone.2008.01.017
37. Hung VW, Zhu TY, Cheung WH, Fong TN, Yu FW, Hung LK, Leung KS, Cheng JC, Lam TP, Qin L (2015) Age-related differences in volumetric bone mineral density, microarchitecture, and bone strength of distal radius and tibia in Chinese women: a high-resolution pQCT reference database study. Osteoporos Int 26(6):1691–1703
38. Kawalilak CE, Johnston JD, Olszynski WP, Kontulainen SA (2014) Characterizing microarchitectural changes at the distal radius and tibia in postmenopausal women using HR-pQCT. Osteoporos Int 25(8):2057–2066
39. Vico L, van Rietbergen B, Vilayphiou N, Linossier MT, Locrelle H, Normand M, Zouch M, Gerbaix M, Bonnet N, Novikov V, Thomas T, Vassilieva G (2017) Cortical and trabecular bone microstructure did not recover at weight-bearing skeletal sites and progressively deteriorated at non-weight-bearing sites during the year following international space station missions. J Bone Miner Res 32(10):2010–2021
40. Seeman E, Delmas PD (2006) Bone quality--the material and structural basis of bone strength and fragility. N Engl J Med 354:2250–2261
41. Amstrup AK, Jakobsen NF, Moser E, Sikjaer T, Mosekilde L, Rejnmark (2016) Association between bone indices assessed by DXA, HR-pQCT and QCT scans in post-menopausal women. J Bone Miner Metab 34(6):638–645
42. Burrows M, Liu D, Moore S, McKay H (2010) Bone microstructure at the distal tibia provides a strength advantage to males in late puberty: an HR-pQCT study. J Bone Miner Res 25(6):1423–1432
43. Alvarenga JC, Boyd SK, Pereira RMR (2018) The relationship between estimated bone strength by finite element analysis at the peripheral skeleton to areal BMD and trabecular bone score at lumbar spine. Bone 117:47–53
44. Manske SL, Liu-Ambrose T, Cooper DM, Kontulainen S, Guy P, Forster BB et al (2009) Cortical and trabecular bone in the femoral neck both contribute to proximal femur failure load prediction. Osteoporos Int 20(3):445–453
45. Boutroy S, Walker MD, Liu XS, McMahon DJ, Liu G, Guo XE, Bilezikian JP (2014) Lower cortical porosity and higher tissue mineral density in Chinese American versus white women. J Bone Miner Res 29(3):551–561
46. Putman MS, Yu EW, Lee H, Neer RM, Schindler E, Taylor AP, Cheston E, Bouxsein ML, Finkelstein JS (2013) Differences in skeletal microarchitecture and strength in African American and white women. J Bone Miner Res 28(10):2177–2185